Optica Applicata, Vol. XLIII, No. 1, 2013
DOI: 10.5277/oa130118

Properties of hydroxyapatite layers used for implant coatings

AGATA DUDEK[1*], LIDIA ADAMCZYK[2]

[1]Institute of Materials Engineering, Częstochowa University of Technology, Armii Krajowej 19, 42-200 Częstochowa, Poland

[2]Division of Chemistry, Częstochowa University of Technology, Armii Krajowej 19, 42-200 Częstochowa, Poland

[*]Corresponding author: dudek@wip.pcz.pl

Metallic materials such as titanium and titanium alloy generally show good mechanical properties but their biocompatibility is limited. In order to manufacture implants which combine improved mechanical properties of metallic material with biotolerance of ceramics, hydroxyapatite coatings are applied. In this paper, plasma sprayed coatings (deposited on titanium Ti–6Al–4V ELI alloy) were analysed. The phase composition of hydroxyapatite (HA) coatings can be determined using a number of methods. The most commonly used are Joel 5400 scanning microscope, scratch test, X-ray diffraction and Raman. The increase of the zirconium and aluminium phase significantly affects the coating adhesion, estimated by the scratch test technique.

Keywords: hydroxyapatite, coatings.

1. Introduction

Joint replacements can be categorised according to the method of fixation used: either cemented or cementless. Cemented implants are fixed using the acrylic cement (PMMA – polymethylmethacrylate cement). It has been used in surgery for the fixation of prostheses for about 40 years [1–4].

The cementless design is a porous implant. The intent is, through biologic fixation, that bone grows into and through the pores in the implant, thereby securing it. In theory the cementless joint replacements are expected to reduce the chance of infection and loosening of the prosthesis, which are the two major complications of hip replacement surgery. The main reasons for failure of uncemented implants are dislocation (31%), aseptic loosening (19%) and infection (11%) [1–7].

Hydroxyapatite (HA) is often used in hip, knee and other implants and as a synthetic bone substitute because it allows for cementless implants and it helps promote bone ingrowth. As time passes, dental and orthopaedic implants coated with HA show

a greater success rate in terms of the overall function of the implant. HA coatings are unique in that they are capable of connecting structurally and functionally with human bone [1–5].

Hydroxyapatite is a calcium phosphate bioceramic material which has an almost identical chemical composition to that of the mineral component of bone. It has excellent biocompatibility and is osteoconductive, allowing bone cells to grow on its surface. The ideal HA coating for orthopaedic implants would be one with low porosity, strong cohesive strength, good adhesion to the substrate, a high degree of crystallinity and high chemical purity and phase stability [3].

A variety of coating techniques have been explored to develop thin coatings of HA, such as plasma-spray technique, pulsed laser deposition, electrodeposition, sol–gel processing and radio-frequency magnetron sputtering. Of the techniques outlined above, only thermal spraying, in particular, is the only commercially accepted method for producing hydroxyapatite coatings. Many research works concern determination of the most optimal conditions of spraying and their impact on the creation of hydroxyapatite coating. Loosening of HA coated implants is generally related to dissolution or delamination of the HA coating. In an implanted prosthesis, the stability and the adherence of implant/coating and coating/bone interfaces strongly affect its performance. Various materials: $Ca(OH_2)$, YSZ (yttria stabilized zirconia), glass, titanium, FA (fluoroapatite), *etc*., have been added to HA to improve the final coating characteristics. Adding reinforcing agent into the hydroxyapatite coating is a possible approach to the reduction of the low properties in interface coating/substrate [6–9].

YSZ (yttria stabilized zirconia) and Al_2O_3 have been commonly used as reinforcement for many ceramics because of their high strength and fracture toughness. Bioinertness is another merit of these materials [10].

2. Materials

The samples with 25 mm diameter and 5 mm thickness were cut from Ti–6Al–4V ELI titanium alloy. The surfaces of titanium pills were then subject to sandblast cleaning and plasma spraying. To create coatings, two types of powder were used (powders showed regular, spherical grain shape):

– HA characterized by high level of purity (Pb = 0.8 ppm, As < 1.0 ppm, Cd, Hg < < 0.1 ppm) and the ratio of Ca/P = 1.67, with mean particle size of 30 μm;

– Zirconium oxide ZrO_2 modified with 8 wt% Y_2O_3 (YSZ – yttria stabilized zirconia) with mean particle size of 30 μm;

– Aluminium oxide Al_2O_3 – 99% purity, with mean particle size of 30 μm.

Bioceramic coatings were deposited on a titanium base by means of plasma spraying, which, due to their undoubted advantages, is the most popular method used for implants.

It was found during the investigations that the most optimal parameters of the process of spraying which allow for obtaining coatings with thickness of 120 μm

are: voltage $U = 55–60$ V, current intensity $I = 500–550$ A, gas flow rate: argon – 3 m^3/h, H_2 – 0.5 m^3/h, distance of the nozzle from sample surface 20–25 cm.

As a result of spraying, the HA coatings and HA coatings with different addition of ZrO_2 and Al_2O_3 phase were obtained according to the following proportions (YSZ – zirconium oxide stabilized with addition of Y_2O_3):

- 100% HA;
- 72% HA + 18% YSZ + 10% Al_2O_3;
- 54% HA + 36% YSZ + 10% Al_2O_3;
- 45% HA + 45% YSZ + 10% Al_2O_3.

3. Methodology

Microstructure testing of the coatings obtained was carried out using Joel 5400 scanning microscope.

Phase composition testing of the coatings used was conducted by means of Raman spectroscopy. To achieve this, a Raman spectrometer (EZ Raman-L Enwave Optronics, Irvine, CA, USA) was used; inducing laser wavelength: 785 nm, laser power: 50 mW.

In order to determine phase composition in the samples obtained, Seifert XRD 3003 X-ray diffractogram with Co lamp with wavelength 0.17902 nm was employed. The measurements were taken with consideration of the following diffractometer parameters: voltage – 40 kV, current intensity – 30 mA, measurement step – 0.1°, impulse count time – 10 s.

The goal of surface geometry and the parameters were determined during examinations by means of Hommel T1000 profilometer. The profilometer allows for the determination of the parameters of surface roughness with accuracy of 0.01 μm.

Adhesion tests for the coatings were carried out by means of Revetest XPress Plus device with Rockwell indenter. The tests were carried out using the following parameters: load of 1 to 200 N, scratch length – 10 mm, scratch rate – 1.89 mm/min.

4. Results and analysis

In order to investigate the impact of addition of ZrO_2 zirconia phase (modified with 8 wt% Y_2O_3) and Al_2O_3 on the structure and mechanical properties of the coating, the coatings were prepared with different content of ZrO_2 (18, 36, 45 wt%) and Al_2O_3 (10 wt%).

The structure and microstructure of the sprayed coatings were revealed by means of a scanning microscope. The example images of the microstructures are presented in Figure 1.

Microscopic observations of the sprayed coatings revealed a structure typical of the employed method of manufacturing. These coatings were characterized by laminarity and porosity between individual layers of solidifying material. Furthermore,

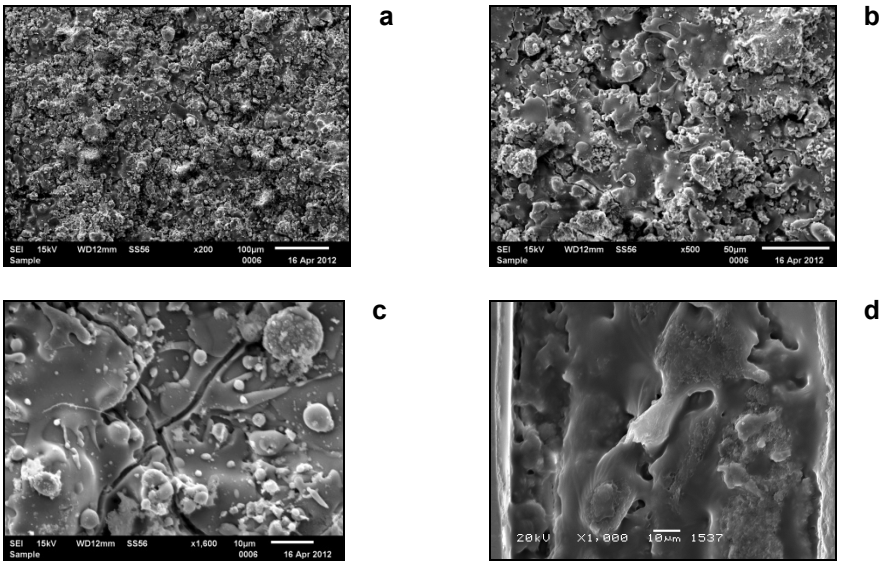

Fig. 1. Microstructure of the surface of ceramic coatings (**a**, **b**, **c**); cross-section of bioceramic coatings (**d**).

the surface showed non-melted or partially melted particles or cracking. During plasma spraying, when the particles reach the substrate they are generally partially molten, consisting of a molten portion and an unmelted core. The final coating thus contains the crystalline phase from the unmelted core and either recrystallised or amorphous phase from the molten portion of the particle. The crystallinity of a HA coating thus depends on the degree of melting of the powder particles within the plasma flame and on the particle cooling rate [8, 9].

Porosity in thermal spray coatings can be in the form of open pores, which are open to the atmosphere, and closed pores, present within the coating itself with no connection to the surface. The sprayed coatings showed comparable porosities of 8–12% regardless of the employed proportions of each powder used for their preparation (HA, ZrO_2 and Al_2O_3).

X-ray structural analysis (Fig. 2) revealed in 100% HA coatings, the presence of the following phases: HA, small content of CaO and amorphous phase. It has been assumed that coatings comprised HA crystalline phase with hexagonal structure of the following cell unit parameters: $a = b = 9.418$ nm, $c = 6.884$ nm and spatial group of $P63/m$. X-ray quantity analysis revealed that the amount of crystalline phase in the coating obtained from 100% powder of HA is at the level of *ca*. 80%. As regards the presence of CaO, one can conclude that HA decomposition occurred and, in consequence, the presence of tricalcium phosphate (TCP) and tetracalcium phosphate (TTCP) phases cannot be entirely excluded (the amount below the X-ray method detection threshold).

In the coatings with addition of zirconium and aluminium phase, the presence of HA, CaO, tetragonal modification of ZrO_2 and α-Al_2O_3 was observed.

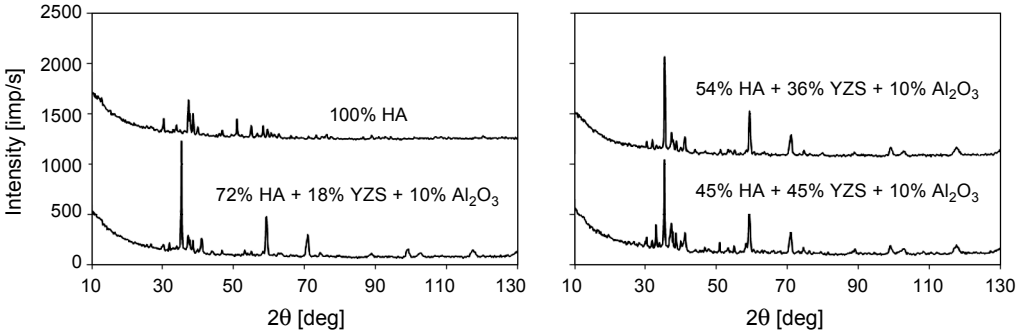

Fig. 2. X-ray diffractograms of the investigated coatings.

The comparison of the results of X-ray tests and Raman spectroscopy allowed to assess the internal structure in the coatings used for investigations. It was revealed that the thermal decomposition of HA into tricalcium phosphate (TCP), amorphous calcium phosphate (ACP), tetracalcium phosphate (TTCP), CaO and other phases, occurred in a very small range within the melted portion of the sprayed particle during the thermal spray process. The Raman spectrum of coatings is given in Fig. 3. This figure shows the phosphate vibration modes region and a particular attention is given to the most intense vibration nondegenerate mode ν_1 near 960 cm^{-1}, corresponding to the symmetric stretching of the P–O bonds, characteristic of the HA layer deposited at the surface of the specimens. The Raman spectrum obtained displays the following bands from phosphate phase PO_4: 432, 443, 577, 590, 604, 1028, 1042 cm^{-1}. The Raman spectra show the typical absorption peaks of α-Al_2O_3, t-ZrO_2. The α-Al_2O_3 gives rise to Raman modes with Raman intensity with peaks at 417, 546, 630 cm^{-1} observed in specimens. The characteristic peaks for a ZrO_2–Al_2O_3 solid solution are absent. Thus, we can conclude from the analysis that there is no solid-solution formation. However, the presence of oxygen vacancies cannot be ruled out. It may be noted here that oxygen vacancies are required for the stabilization of the cubic phase, and they do lead to a stable tetragonal phase t-ZrO_2 (which appear at around 461, 602, 648 cm^{-1}).

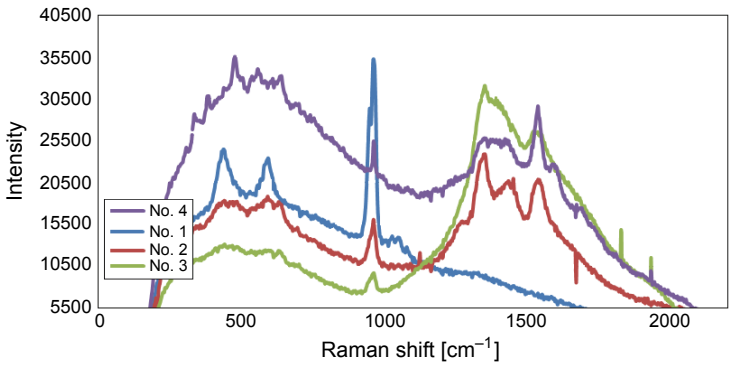

Fig. 3. Raman spectrum for coatings.

The roughness of the coating is affected by the size of the particles used for plasma spraying. GROSS and BABOVIC [11] found that partially melted particles were not able to flatten on the coating surface giving rise to large undulations and thus higher coating roughness. HA powder particles with an average size 30 μm were found to give a coating roughness of 4 to 6 μm. High surface roughness values lead to a greater coating dissolution rate. The optimal value for coating roughness is still unclear. The results obtained for individual coatings are presented in Table 1.

T a b l e 1. Roughness parameters of the coatings.

Specimens	Ra [μm]	Rmax [μm]	Rz [μm]	Rt [μm]	Rp [μm]	RSm [μm]
100% HA	5.50	34.16	32.01	38.55	21.57	89.0
72% HA + 18% YZS + 10% Al_2O_3	5.71	46.34	28.71	48.93	28.04	88.9
54% HA + 36% YZS + 10% Al_2O_3	5.44	40.84	29.86	42.16	20.14	77.6
45% HA + 45% YZS + 10% Al_2O_3	5.45	38.89	32.76	41.45	19.24	87.1

where: Ra – arithmetic average of the roughness profile, Rmax – maximum distance between the peak and dip, Rz – maximum height of the profile, Rt – total height of the profile, Rp – maximum peak height, RSm – mean width of the valley in the profile.

A very essential parameter for industrial customers for implants with HA coating is a development of the surface in sprayed coatings defined with arithmetic average of the roughness profile, *i.e.*, average roughness Ra.

The parameters of geometrical structure obtained for all the studied coatings were comparable. The addition of zirconium and aluminium phase to HA ceramics did not considerably affect the roughness of the coatings.

The main purpose of the investigations was to obtain a characteristics of mechanical properties on the coating–implant interface (Fig. 4). This characteristics was obtained through the analysis of the force of adhesion to the base materials and

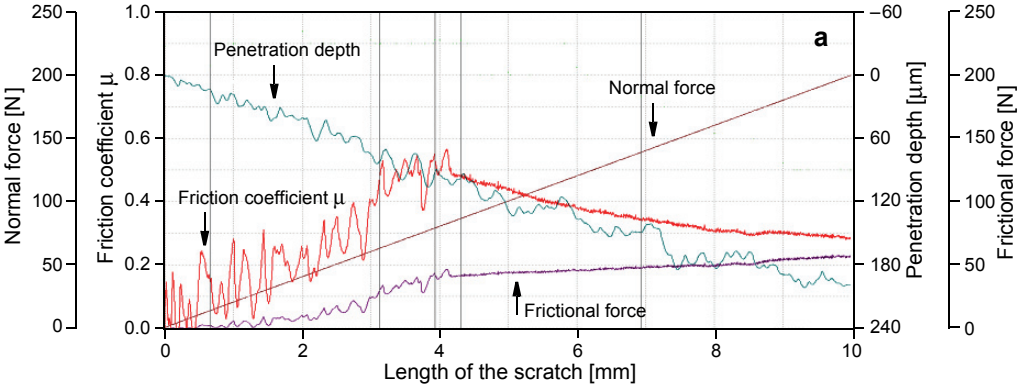

Fig. 4. To be continued on the next page.

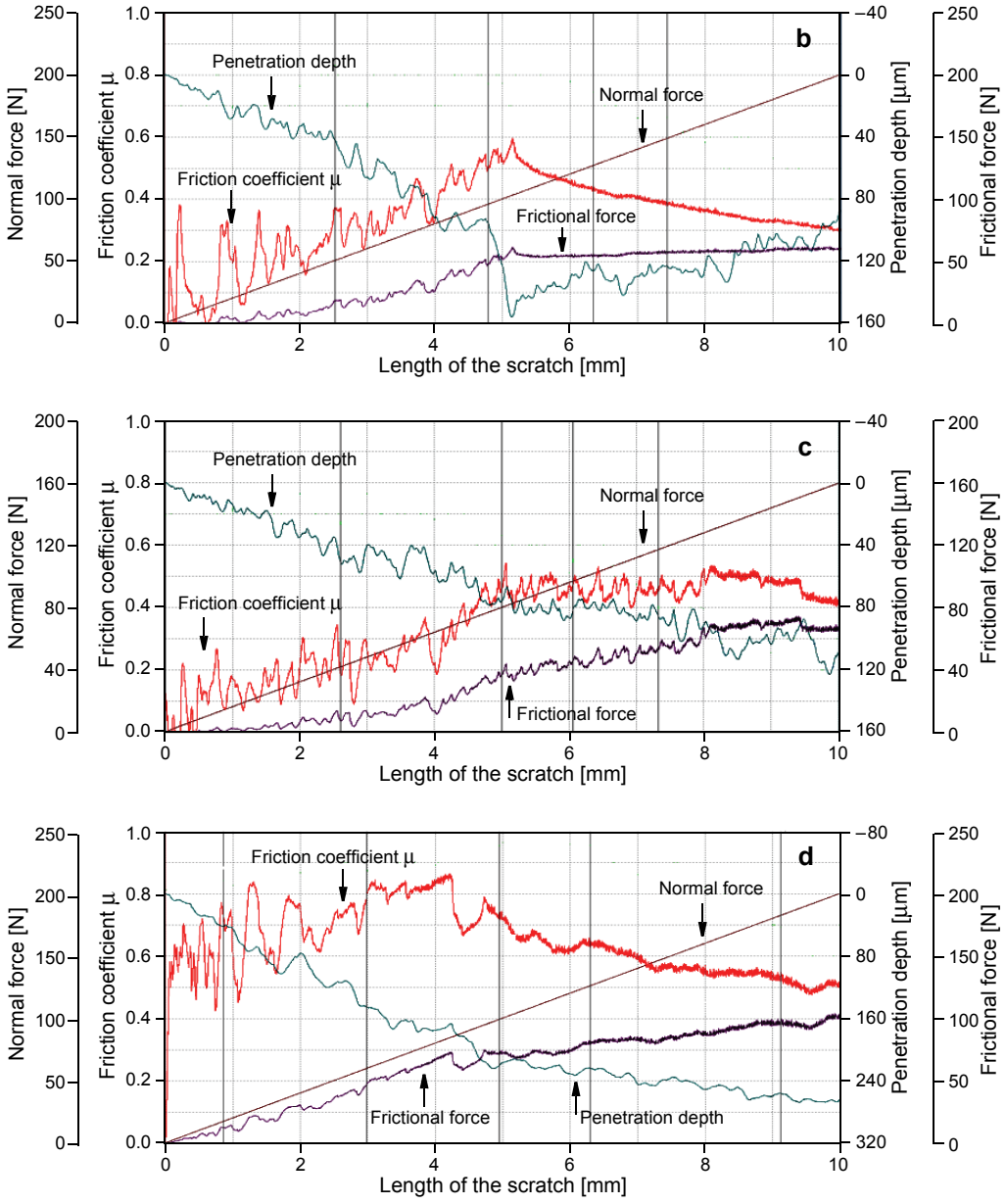

Fig. 4. Charts obtained as a result of scratching: **a** – 100% HA (L_{krit} = 84 N), **b** – 72% HA (L_{krit} = 106 N), **c** – 54% HA (L_{krit} = 142 N), **d** – 45% HA (L_{krit} = 147 N).

the analysis of cracking and deformations as well as calculations of such parameters as: force, friction coefficient and critical force. The investigations encompassed hydroxyapatite layers with thickness of *ca*. 120 μm obtained by means of plasma spraying. The depth of the scratched area (its linear dimensions) was closely dependent

on the adopted test parameters. A rise in the used force caused changes in the scratch line profile. The adjacent surfaces (*i.e.*, indenter–coating) were in a complex state of stresses and deformations, which caused that each of the investigated coatings reached critical value.

The investigations of adhesion force in bioceramic coatings allowed to characterize the coating/base material system [HA(YZS + Al_2O_3)/Ti–6Al–4V] through the analysis of the values such as: friction coefficient, friction force, critical load force for the coatings at which they were separated. The addition of zirconium and aluminium oxide had an impact on the rise in critical force at which the coating separated from the base material. In the case of 45% addition of ZrO_2, the value of the force accounted for *ca*. 75% as compared to 100% HA coating.

5. Conclusions

As a result of plasma spraying, a 120 μm thick hydroxyapatite coating was obtained with different additions of modified zirconium and aluminium oxide. The analysis of microstructures revealed the structures typical of sprayed coatings, *i.e.*, laminarity, porosity and presence of non-melted or partially-melted particles of the powders.

The analysis of HA+YSZ+Al_2O_3 coatings reveals that the addition of zirconium and aluminium phase insignificantly reduces the amount of amorphous phase after the process of spraying (the amount of crystalline phase rises to *ca*. 95%).

X-ray structural and Raman analysis confirmed high thermal stability of the hydroxyapatite powder used. The presence of YSZ and Al_2O_3 phase in the composites under investigation did not show considerable effect on decomposition of HA phase.

The increase in zirconium and aluminium phase significantly affects the coating adhesion, estimated by the scratch test technique.

References

[1] JARCHO M., *Calcium phosphate ceramics as hard tissue prosthetics*, Clinical Orthopaedics and Related Research **157**(), 1981, pp. 259–278.
[2] DE GROOT K., *Bioceramics of Calcium Phosphate*, CRS Press, Boca Raton, Vol. 146, 1983, pp. 1–32.
[3] DE GROOT K., *Bioceramics consisting of calcium phosphate salts*, Biomaterials, **1**(1), 1980, pp. 47–50.
[4] AOKI H., KATO K., *Studies on the application of apatite to dental materials*, The Journal of Dental Engineering **18**, 1977, pp. 86–89.
[5] CHENGKANG CHANG, JINGQI HUANG, JIYU XIA, CHUANXIAN DING, *Study on crystallization kinetics of plasma sprayed hydroxyapatite coatings*, Ceramics International **25**(5), 1999, pp. 479–483.
[6] BHADANG K.A., GROSS K.A., *Influence of fluorapatite on the properties of thermally sprayed hydroxyapatite coatings*, Biomaterials **25**(20), 2004, pp. 4935–4945.
[7] HONG LIANG, BING SHI, FAIRCHILD A., CALE T., *Applications of plasma coatings in artificial joints: An overview*, Vacuum **73**(3–4), 2004, pp. 317–326.
[8] DUDEK A., *Microstructure and Properties of the composites: Hydroxyapatite with addition of zirconia phase*, Journal of Engineering Materials and Technology **133**(2), 2011, article 021006.

[9] DUDEK A., *Surface properties in titanium with hydroxyapatite coatings*, Optica Applicata **39**(4), 2009, pp. 825–831.
[10] PICONI C., MACCAURO G., *Zirconia as a ceramic biomaterial*, Biomaterials **20**(1), 1999, pp. 1–25.
[11] GROSS K.A., BABOVIC M., *Influence of abrasion on the surface characteristics of thermally sprayed hydroxyapatite coatings*, Biomaterials **23**(24), 2002, pp. 4731–4737.

Received May 25, 2012
in revised form October 4, 2012